2D-IR spectroscopy of azide-labeled carbohydrates in H_2O

P. Gasse, T. Stensitzki, and H. M. Müller-Werkmeister*

University of Potsdam, Institute of Chemistry, Physical Chemistry, Karl-Liebknecht-Str. 24-25, 14 667 Potsdam, Germany

(*Electronic mail: henrike.mueller-werkmeister@uni-potsdam.de)

(Dated: 24 June 2024)

Carbohydrates constitute one of the key classes of biomacromolecules, yet vibrational spectroscopic studies involving carbohydrates remain scarce as spectra are highly congested and lack significant marker vibrations. Recently, we introduced and characterized a thiocyanate-labeled glucose[1] demonstrating the use of vibrational reporter groups for 2D-IR spectroscopy of carbohydrates. Here, we expand upon those results and elucidate the performance of azide groups as vibrational reporter for carbohydrates. Originating from applications in click-chemistry, different azide-labeled carbohydrates are readily available. We have characterized azide-labeled glucose, galactose, acetylglucosamine and lactose in water using IR and 2D-IR spectroscopy. Our findings indicate that their absorption profiles are primarily determined by the labeling position on the ring. However, we also observe additional variations between samples with the same labeling position. Furthermore, we demonstrate that their usage remains feasible at biologically relevant concentrations.

I. INTRODUCTION

The use of vibrational reporter groups for studies of biomolecules has emerged as a key tool in the domain of two-dimensional infrared (2D-IR) spectroscopy[2,3]. Recently, we presented a glucose[1] labeled with thiocyanate (SCN) as a vibrational reporter group, making use of the same spectrally free window known for proteins[4]. In the present study, we test the use of azide moieties as vibrational labels for carbohydrates. Azide labels are broadly used as reporter groups in several FTIR and 2D-IR studies[5–13] and are herein applied to a diverse selection of carbohydrates, as shown in Figure 1. Unlike the previously presented SCN-labeled carbohydrate, all characterized sugars are available commercially, driven by applications in click chemistry.

Azides are attractive as vibrational probes due to their much higher extinction coefficient[14] in contrast to thiocyanate or nitriles. They exhibit strong sensitivity to their immediate environment, with both hydrogen bonding and electrical field contributing to spectral changes[15]. However, we acknowledge the challenges posed by their short vibrational lifetime[5] and potential Fermi resonances[16], which may hinder the interpretation of the signal. Furthermore, the complex solvatochromism[17] of the azide group inhibits its use as a direct probe of the local electric field.

For this study we have selected azide-functionalized glucose and galactose as representative monosaccharides with huge relevance in physiological processes, i.e. the glucolytic metabolic pathways or brain development[18].

In addition to the examination of basic monosaccharides, our investigation extends to the investigation of two azide-functionalized carbohydrates with heightened biochemical significance and more chemical complexity. First, we selected N-Acetylglucosamine (GlcNAc), which is an ubiquitious constituent of complex bioactive glycopolymers in all cellular systems, such as hyaloronic acid, found in the extracellular matrix, peptidoglycan or chitin, constituents of cell walls and exoskeletons respectively[19]. As substantial part of glycans (complex polysaccharides linked glycosidically) it is involved in processes like cell signaling[20], immune response[21], and protein function[22], all which may be addressed with azide carbohydrates. Second, we selected lactose, comprised of glucose and galactose moieties as representative disaccharide. Lactose constitutes the primary source of energy within maternal lactation. It undergoes specific enzymatic hydrolysis mediated by the enzyme lactase[23].

The azide label can be attached to different positions on the carbohydrate ring. How this influences the spectral features is not immediately clear and needs to be quantified. To elucidate the sensitivity of the vibrational label, we compare distinct label positions on C_2- and C_6-labeled glucose, as well as the comparison between C_6-labeled glucose and galactose. The latter pair differs solely in the conformational arrangement of the hydroxyl (OH) group at the C_4 position.

We assess the performance of the vibrational reporter groups by using FTIR and 2D-IR spectroscopy, providing insights into the ultrafast structural dynamics of those carbohydrates. The use of 2D-IR signals permits the identification of spectral fluctuations and the subsequent characterization of distinct sub-populations of the labelled carbohydrate derivates.

Our results show that the labeling position has a strong influence on the spectra, resulting in both shifts in position and changes in shape. Further differences are still observed between samples with the same position, showing an additional sensitivity to the sugar itself. For the C_2-labeled galactose, we observe a rather narrow band along with an unusually long vibrational lifetime, suggesting limited solvent interaction. In four out of fives samples, we observe an offset in the center line slope (CLS)-decay, indicating the presence of sub-populations not exchanging within the vibrational lifetime.

II. MATERIALS AND METHODS

A. Investigated carbohydrates

The structures of the examined carbohydrates are depicted in Figure 1. All samples were ordered from Sigma-Aldrich

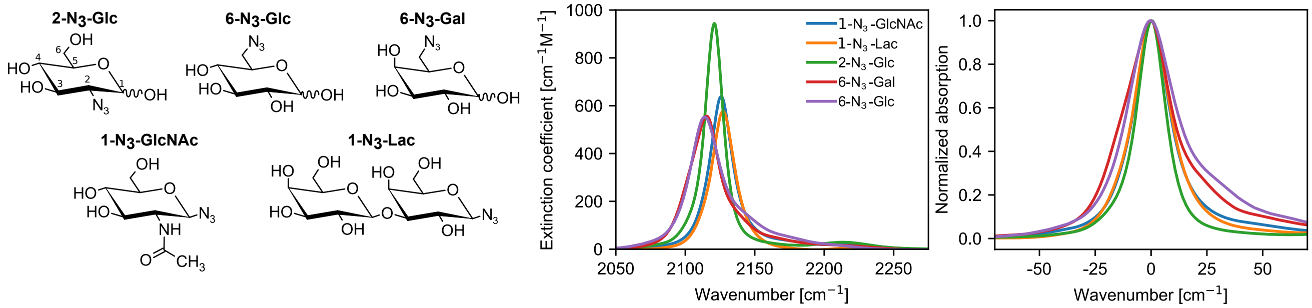

FIG. 1. *Left*: Structures of the investigated azide carbohydrates. The numbers at the top left structure indicate the numbering of ring carbon atoms. *Middle*: Background corrected FTIR spectra of the N_3-stretching vibration of the investigated compounds in water. *Right*: Peaks have been normalized and overlaid for better comparison of the peak shapes.

and had a purity $\geq$95%. They can be categorized into two distinct groups. Firstly, there are the monosaccharides, which are only modified via the introduction of an azide group: specifically, 2-deoxy-2-azido-glucose (2-N_3-Glc), 6-deoxy-6-azido-glucose (6-N_3-Glc), and 6-deoxy-6-azido-galactose (6-N_3-Gal). The azide group is positioned at either the C_2 or C_6 position. These samples can exist in two isomeric forms, α and β, contingent upon the conformational orientation of the hydroxyl (OH) group at the C_1 position. The second group includes two more complex carbohydrates: 1-deoxy-1-azido-N-acetylglucosamine (1-N_3-GlcNAc) with an acetamide group at the C_2 postion and the disaccharide 1-deoxy-1-azido-lactose (1-N_3-Lac), both with the azide group at C_1.

B. Sample Preparation

All samples were dissolved in H_2O (milli-Q water) for the purpose of IR spectroscopic measurements. The specimens were prepared within a calcium fluoride (CaF_2) sandwich cell. The spacer thickness was 25 µm for 1-N_3-GlcNAc and 1-N_3-Lac, and 50 µm for 2-N_3-Glc, 6-N_3-Glc and 6-N_3-Gal.A concentration of 400 mM was used across all samples to record FTIR spectra. For 2D-IR spectroscopy, we used different concentrations: 400 mM for 1-N_3-GlcNAc and 1-N_3-Lac. 100 mM for 2-N_3-Glc, 6-N_3-Glc and 6-N_3-Gal.

C. FTIR

FTIR spectra were acquired at ambient temperature (21 °C) with a Tensor II FTIR spectrometer (Bruker), equipped with a liquid nitrogen-cooled mercury cadmium telluride detector. Each spectrum, spanning from 800 cm^{-1} to 4000 cm^{-1}, was generated by averaging 256 interferograms with a spectral resolution of 2 cm^{-1}. Fourier transformation was executed employing a Blackmann-Harris apodization function and a zero-filling factor of 1.

To remove water-related signals underlying the N_3-signal, a twofold correction approach has been used. A pure water spectrum (pertaining to N_3-Glc/N_3-Gal) was subtracted from the experimental data. For the 1-N_3-GlcNAc/1-N_3-Lac samples a ninth-order polynomial function was applied to model and remove the water combination mode contributing to the background.

D. Time-resolved IR and 2D-IR spectroscopy

The 2D-IR setup employed herein is as previously detailed in reference[1]. The pump pulse (FWHM of 500 cm^{-1} and central wavenumber at 2150 cm^{-1}) energy at the sample was 2 µJ, with a focus smaller than 60 µm FWHM. During the measurement of 1-N_3-GlcNAc, the data was influenced by scattering effects, which were effectively mitigated by computing the mean of six spectra that exhibited solely scattering and no discernible signal. Initially, the 2D-IR signal of 2-N_3-Glc, 6-N_3-Glc and 6-N_3-Gal had a artifact, showing up as stripes along the pump axes proportional to 2D-IR signal. We minimized the artifact by reducing the multiplication factor of the interferrogram spectrum at $t_1 = 0$ fs below the default 0.5[24]. In all cases, we found a factor about 0.27 to 0.4 ideal (see SI). We guess, the artifact is caused by multi-photon absorption occurring only when the pulse arrives together, but not otherwise.

Data analysis was performed with skultrafast package[25]. For the determination of the center line slope (CLS) we used a window of $\pm$11 cm^{-1} centered around the maximum of the ground state bleach for the pump axis, resulting in five datapoints, and a window of $\pm$10 cm^{-1} for the probe axis. The inhomogeneous line broadening was determined by a diagonal and anti-diagonal cut through the ground state signal at 100 fs. A pseudo-Voigt profile was fitted to the part of the cut containing only negative signals, from which the full-width-half-maximum (FWHM) was extracted (see SI). The difference between their FWHMs is yielding the inhomogeneous line-broadening. The anharmonicity was determined by measuring the distance between positive and negative maxima at the pump-slice with the largest amplitude.

III. RESULTS AND DISCUSSION

A. FTIR spectroscopy

The FTIR spectra of the asymmetric stretching vibration of the azide-labels are presented in figure 1. Their spectra are mainly modulated by the labeling position, but small differences are still observed between samples with the same label position (see table I); i.e. for 6-N_3-Gal and 6-N_3-Glc we can resolve differences in the spectral position and line shape, although they are rather small. We attribute the differences to differing electric field and hydrogen bond environments surrounding the azide oscillator[15,17,26,27]. Therefore, owing mostly to the labeling position, the azide interacts to different amounts with the solvent and or the intrinsic carbohydrate structure. Interestingly, the herein observed absorption maxima span the whole range of those previously reported[6,11,14,28–30] frequencies in water of 2115 cm^{-1} to 2124 cm^{-1}, again highlighting the influence of the labeling position.

Sample	ν_{max}	FWHM	$\varepsilon(\nu_{max})$	$\int \varepsilon(\nu)d\nu$
1-N_3-GlcNAc	2125.7	19.3	647	17 600
1-N_3-Lac	2127.2	19.3	594	14 200
2-N_3-Glc	2120.7	15.7	921	21 500
6-N_3-Gal	2115.7	26.4	551	20 100
6-N_3-Glc	2114.3	27.1	550	21 900

TABLE I. The position ν_{max} (cm^{-1}), FWHM (cm^{-1}), peak extinction coefficient $\varepsilon(\nu_{max})$ ($L\,mol^{-1}\,cm^{-1}$) and integrated extinction coefficients ($L\,mol^{-1}$) for all measured samples.

The FHWM values (see table I) also fall into the three groups, again one for each labeling position. The narrowest peak is observed for 2-N_3-Glc. 1-N_3-GlcNAc and 1-N_3-Lac exhibit a 4 cm^{-1} broader peak and the samples labeled at C_6 an additional broadening of at least 10 cm^{-1} relative to the 2-Glc peak.

The broader peaks are accompanied by more complicated shapes. The azide groups in the C_1 and C_2 positions display only small shoulders. Their main peak can be well described using a single pseudovoigt function. In contrast, the peak structure of the C_6-labeled samples is more complex and exhibits multiple shoulders.

Lately we proposed that the spectral shoulders of the SCN-labeled carbohydrates to be sourced by stable structural subpopulations due to the rotational freedom of SCN[1]. While azide and thiocyanate can in principle both rotate around the C-N(NN) respectively the C-S(CN) bond, it seems that azide has no substantial double peak structure when placed right at the carbohydrate ring at the positions C_1 or C_2. For these, the azide label is situated directly at the carbohydrate ring and exhibits limited flexibility, since rotational motion is hindered by the neighboring hydroxy groups. Consequently, it interrogates a more homogeneous molecular environment compared to azides located at the C_6 position of the molecule, which gain significant rotational freedom for the C-N bond due to their indirect attachment to the ring structure. We assume that the increased rotational freedom manifests as the presence of multiple stable subpopulations within the signals of 6-N_3-Glucose and 6-N_3-Galactose, observed as spectral shoulders.

With the exception of 6-N_3-Glc, all samples exhibit an small absorption at 2220 cm^{-1}, the origin of which remains unclear, as the observed signal exceeds shift that would typically be expected for azides[31]. Since the carbohydrates all show strong bands around 1100 cm^{-1} associated with C-O stretching and H-bending modes, we propose the origin of this band is either the overtone or a Fermi-resonance of one of theses bands.

Lastly, an interesting finding from the FTIR spectra pertains to the relatively high peak extinction coefficient observed, particularly for 2-N_3-Glc, which demonstrates a good capacity to absorb IR light, measuring at 920 $L\,mol^{-1}\,cm^{-1}$. The other samples exhibit $\varepsilon(\nu_{max})$ ranging from 550 $L\,mol^{-1}\,cm^{-1}$ to 650 $L\,mol^{-1}\,cm^{-1}$ (see table I). The particularly high value of 2-N_3-Glc is diminished by the fact that the integral of the extinction coefficient over the entire signal is similar to 6-N_3-Glc and 6-N_3-Glc. The bands of 1-N_3-GlcNAc and 1-N_3-Lac are weaker in comparison. Nevertheless, these are high values when compared to other commonly used labels such as SCN, CN, CD, as reported in prior references[29,32].

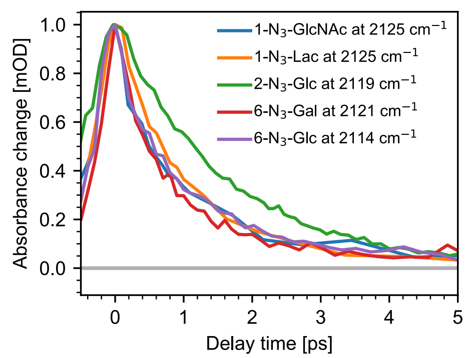

FIG. 2. Normalized transients showing the decay of the excited state absorption as measured by broadband IR pump-probe spectroscopy. With the exception of 2-N_3-Glc, which has a noticeable longer lifetime, all signals decay almost identical.

https://doi.org/10.26434/chemrxiv-2024-51zzb ORCID: https://orcid.org/0000-0001-9471-882X Content not peer-reviewed by ChemRxiv.

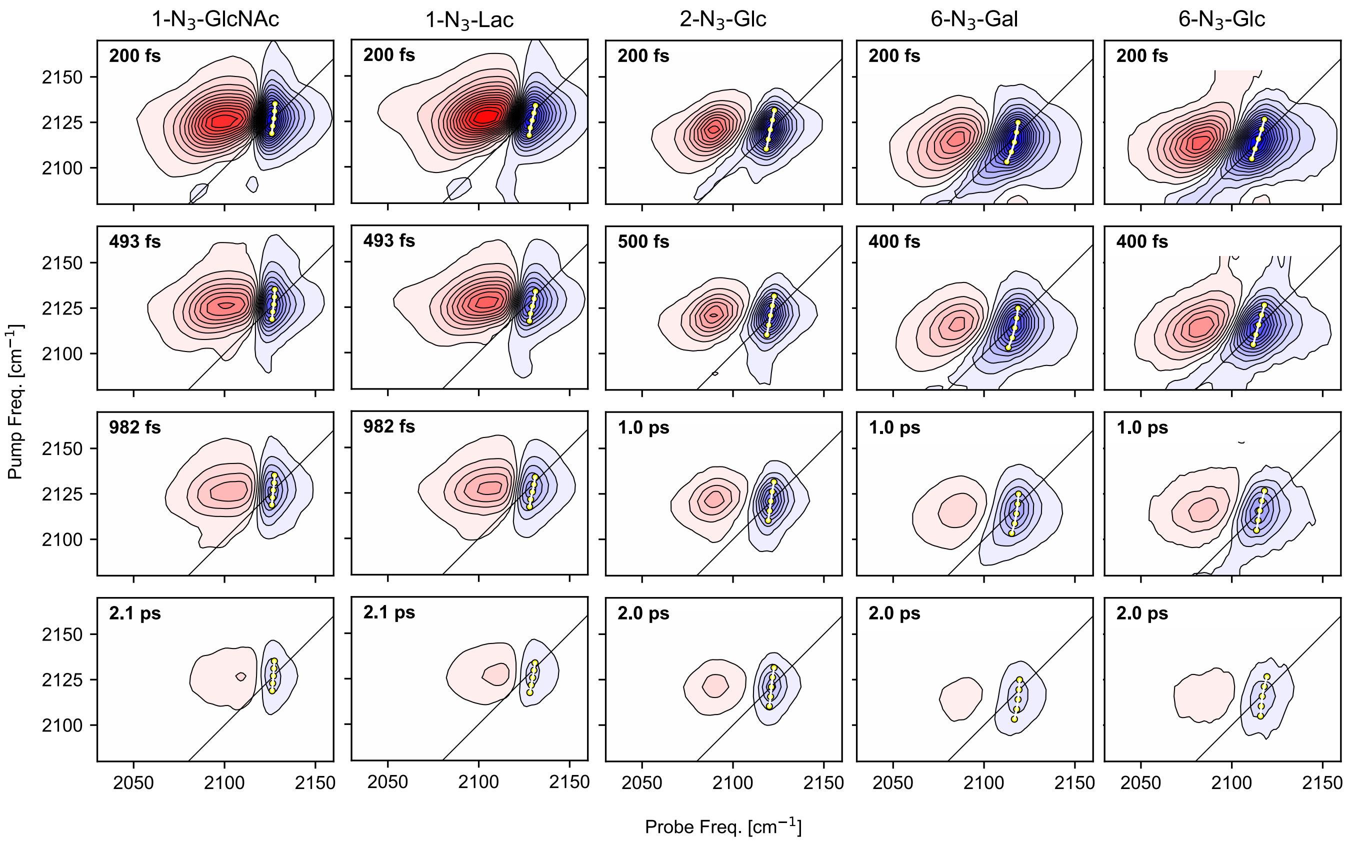

FIG. 3. Contour plots of the 2D-IR spectra of all samples at selected waiting times. The levels are equidistant. Blue color indicates ground state bleach and stimulated emission contributions, red color refers to excited state absorption contributions. The yellow dots show the points used to generate center lines (white lines), which is used for the CLS analysis.

B. Vibrational lifetimes

We conducted IR pump-probe measurements to acquire the vibrational lifetimes associated with the N_3 anti-symmetric stretching vibration. Figure 2 presents the recorded transients. The figure shows that all samples, with exception of 2-N_3-Glc, have almost identical vibrational lifetimes.

For a detailed analysis, the vibrational lifetimes were estimated through a global fitting approach utilizing two exponential functions applied to all data acquired after a delay time of 0.3 ps. The shorter-lived component of the exponential decay reflects the vibrational lifetime, whereas the remaining longer-lived exponential decay is attributed to residual hot-bands (see supporting information). For all tested samples, with the exception of 2-N_3-Glc, the vibrational lifetime was determined to be 1.0 ps. 2-N_3-Glc displayed a considerably distinct behavior, featuring a vibrational lifetime that is 1.5 ps and therefore 50 % longer compared to the other samples. The observation is also in line with observed narrower linewidth of 2-N_3-Glc, suggesting a narrower homogeneous linewidth and therefore a longer lifetime[24]. Furthermore, the lineshape broadening can be attributed almost completely to homogeneous lifetime broadening, as an lifetime of 1.5 ps itself equals to a width of 14.2 cm^{-1}, only slightly smaller than the measured 15.7 cm^{-1}. Similarly, the peaks of the C_1-labeled sugars both have widths near their homogeneous limits of 20.6 cm^{-1}. For the sugars labeled at the C_6-position, the linewidth of the peaks are clearly inhomogeneously broadened, as their lifetime is identical to the C_1-labeled sugars but their spectra are much broader.

These estimated lifetimes align well with previous investigations involving N_3 in aqueous environments[33]. The similarity of lifetimes of all samples except 2-N_3-Glc can be explained by a vibrational decay pathway predominantly involving solvent receptor modes[34–36]. Therefore, we propose that the longer lifetime of 2-N_3-Glc is also caused by a less solvent-exposed position, which can be explained by its structure. While 2-N_3-Glc has two neighbouring OH-groups at the carbohydrate ring, the other samples are more accessible for solvents, as they have only one or no OH-group directly next to them.

The short vibrational lifetime restricts the applicability of azide reporter groups in carbohydrate studies, particularly when investigating dynamics on timescales longer than a few picoseconds. However, Chalyavi et. al[37] showed an approach to extend the lifetime by using isotope labeled N_3, which could also applied here.

C. 2D-IR spectra

Following the observations made in the FTIR findings, we find three categories associated with the label positions also within the 2D-IR spectra. Selected waiting times shown in Figure 3. The C_1-labeled substances, namely GlcNAc and Lactose, exhibit a comparable peak shape, demonstrating a small anharmonicity and a pronounced extension along the pump axes. Similarly, the C_6-labeled compounds, glucose and galactose, also display elongation along the pump axis. The third category is represented by 2-N3-Glc, which possesses the narrowest and most symmetrical signal.

Overall, the anharmonicity, which is depicted in table II, is small compared to the linewidth, leading to overlapping contributions of positive and negative signals, potentially affecting the calculations of the CLS-values and the inhomogeneous line-broadening.

All 2D-IR spectra exhibits a shape similar to other azide samples previously studied[5,11]. As in these studies, the excited-state absorption of the azides measured here is noticeable broader than the ground-state contributions. The broadening deviates from the typical behavior observed in 2D-IR signals, and its underlying origin remains unclear to our knowledge. The broadness of the excited-state absorption is especially pronounced for samples labeled at the C_1-position, which also have a 7 cm^{-1} smaller anharmonicity than the other samples, indicating a linked origin.

We also applied a CLS-analysis of the ground-state bleach to all datasets, shown by yellow points in Figure 3. The resulting slopes and their exponential fit are shown in Figure 4. In line with our earlier observations of that the lineshape is mainly homogeneously broadened, most observed slopes are quite small. In all cases, the amplitude of decay is in the range of 0.2. All samples expect 1-N_3-GlcNAc have an remaining offset at 2 ps. Furthermore, the decay of the CLS seems to be almost non-exponential for the samples labeled at C_1. In particular, an exponential fit of the CLS-decay of 1-N_3-GlcNAc fails.

Still, the observed spectral diffusion times are all in the expected range for azide-labels in water[6,11,38]. The diffusion process on the sub 1 ps scale is mainly attributed to H-bond residence time in water.[38]

Sample	τ_{vib}/ps	τ_1/ps	Δ_1	Δ_∞	Δ_{inh}/cm^{-1}	Anh/cm^{-1}
1-N_3-GlcNAc	1.03(1)	-	-	-	1.3(6)	24
1-N_3-Lac	1.03(1)	1.1(3)	0.20(1)	0.06(2)	2.4(7)	23
2-N_3-Glc	1.48(1)	0.6(1)	0.18(1)	0.09(0)	3.4(3)	31
6-N_3-Gal	1.06(1)	0.7(1)	0.17(1)	0.13(1)	5.9(7)	31
6-N_3-Glc	1.03(1)	0.5(1)	0.24(3)	0.18(1)	5.6(3)	33

TABLE II. Measured values of the vibrational lifetime τ_{vib}, CLS decay time τ_1, amplitude Δ_1, and offset Δ_∞, as well as the inhomogenoues line-broadening at 100 fs Δ_{inh} and the anharmonicity Anh. Errors are shown in parentheses, representing the uncertainty in the last digit.

The origin of the CLS offsets remains unclear. However, the FTIR spectra of the C_6-labeled samples exhibit a distinct shoulder, suggesting the presence of sub-populations that do not exchange on the observed time scale. For 1-N_3-Lac and 2-N_3-Glc, we observe only a weak or no shoulder in the linear spectra, respectively. Despite this, the 2D-IR spectra and the CLS of both samples still show a persistent tilt after 2 ps, indicating a inhomogeneity that is not resolved in the steady-state spectra.

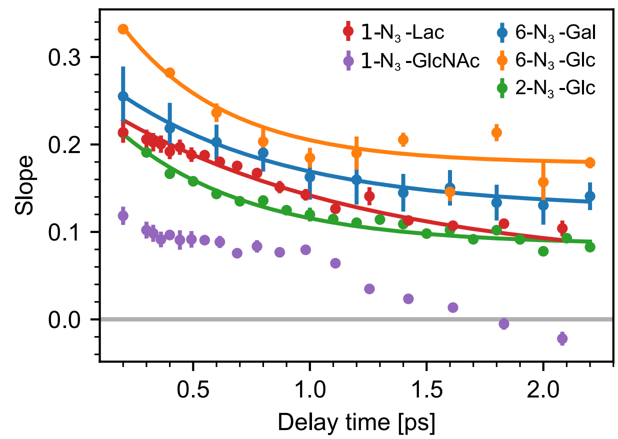

FIG. 4. Center line slopes of the investigated azid-carbohydrates represented by dots. The black lines show the resulting exponential fits of the recorded data. The fitting procedure for 1-N_3-GlcNAc was not successful.

We previously hypothesized[1] that the orientation of the vibrational reporter group influences the spectral properties. For the azides presented here, the vibrational lifetime is too short to fully sample all possible orientations. Additionally, the ring geometry constrains the orientations of the N_3 group, particularly as rotation is hindered by neighboring hydroxy groups. Consequently, different ring geometries affect the spatial exploration of the reporter group. Similarly, the C_2- and C_6-labeled samples can exist in both α and β configurations, impacting the spectra in the same way.

We also determined the inhomogeneous line broadening of the bleaching band from the anti-diagonal and diagonal slices (see Table II). As expected, the line broadening follows the observations of the CLS analysis. The C_6-labeled samples show the largest broadening, while both 2-N_3-Glc and 1-N_3-Lac show only slight broadening. 1-N_3-GlcNAc shows no broadening. These observations are consistent with our earlier findings from the FTIR and lifetime analysis, which indicated that only the C_6-labeled samples are inhomogeneously broadened.

While the measurement of azide carbohydrates in non-biological/biochemical contexts is possible at high concentrations, conducting further investigations of biochemical processes using 2D-IR spectroscopy requires significantly lower concentrations. To determine the use of azide carbohydrates in this context, we tested a 10 mM solution of 2-N_3-Glc. The resulting 2D-IR signals are depicted in Figure 3.

When compared with the 100 mM reference, the 2D-IR signal of the 10 mM sample remains well-resolved. As expected, the signal to noise ratio is lower, but this can be handled with a longer measurement time. Here a single spectra was measured in seven minutes, while we measured the 100 mM sample in two minutes per time point. Both datasets would have been usable with less measurement time. The CLS decay/amplitude

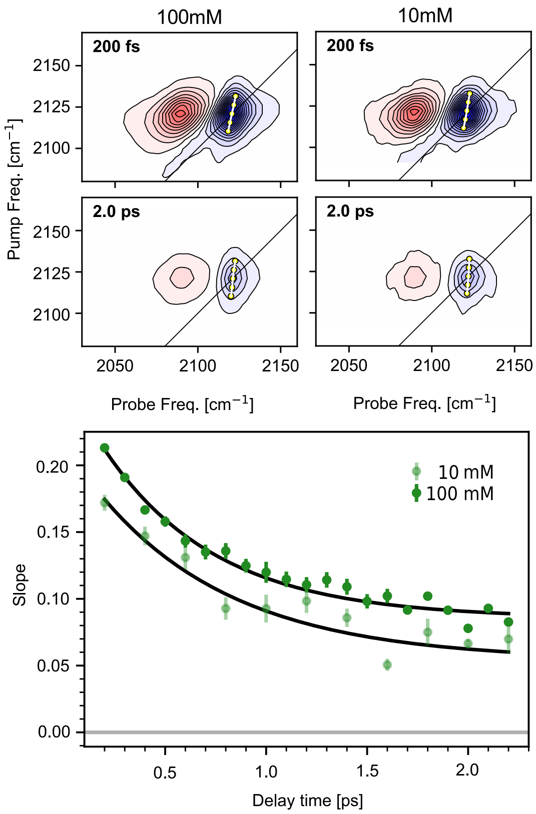

FIG. 5. *Top*: 2D-IR spectra of 2-N_3-Glucose in H_2O at concentrations of 10 mM and 100 mM for selected waiting times. The yellow line in the GSB-signal indicates the center line slope. *Bottom:* CLS-decay of the two concentrations.

and vibrational lifetimes observed in the 10 mM sample are consistent with those of the 100 mM samples. There are small differences in the offset, that might be caused by increased noise or more pronounced systematic errors for the 10 mM data.

It is worth noting that 10 mM is still a relatively high concentration in the context of biological and biochemical research. Particularly in the study of protein-carbohydrate interactions, concentrations typically do not exceed a few mM. However, the successful resolution of the 10 mM signal gives us confidence in our ability to measure even lower concentrations, potentially down to 1 mM or lower. Importantly, the presented experiments were performed in H_2O, rendering solvent exchange to D_2O unnecessary, increasingly valid for protein studies by 2D-IR as well[39].

Furthermore, with modern systems running at 100 kHz[40–43] even sub-millimoloar concentrations should be possible. Using further reduction techniques like sub-sampling with compressed sensing[44] or denoising using neural networks[45] should even allow their application in screening approaches.

IV. SUMMARY & OUTLOOK

The incorporation of azides into carbohydrates yields an efficient vibrational probe, albeit with a limited observable temporal range. Yet we find the signal strength of azide groups superior to other labels, as we find here high extinction coefficients of aliphatic azide groups attached to carbohydrates, which eases detection of signals in 2D-IR spectroscopy.

The sensitivity of the local molecular environment surrounding the azide label is demonstrated through pronounced spectral changes associated with the label position and further small shifts due to the slightly varied carbohydrate structures. Azides attached to the C_1- and the C_2 have mostly symmetric lineshapes. In contrast, labels at the C_6-position show a complex peak-structure with clearly visible shoulder.

Moreover, the azide vibration of C_2-labeled sugar has unique characteristics, it is unusually narrow and has a longer lifetime than the other samples, 1.5 ps instead of 1.0 ps, with latter being typical for azide-labels in water. This suggests, that at this position the solvent interaction is reduced, which can be explained by the additional steric hinderence at C_2 inherent to the pyranose structure.

With the exception of 1-N_3-GlcNAc, all samples show a non-decaying peak tilt in the 2D-spectra, which we observe also as an offset in the CLS-decay. This suggests heterogeneous molecular environments of the azide moieties not exchanging on the observed time-scale. We attribute the sub-populations to different azide orientations and different solvent accessibility, which may be further affected by different ring-configurations. For C_2- and C_6-labeled samples, both α- and β-configuration are in principle possible and therefore could be contributing. However, with the exception of the C_6-labeled samples, the linewidth is primarily due to homogeneous broadening, indicating that the different sub-populations exhibit only slight frequency variations.

In summary, 2-N_3-Glc, 1-N_3-Lac and 1-N_3-GlcNAc exhibit a sharp and symmetric peak structure, alongside favorable extinction coefficients. These compounds can be readily used to address more specific questions, such as the investigation of the lactose/lactase enzymatic reaction using 1-N_3-Lac, or the complexity of glycan structures using 1-N_3-GlcNAc.

Overall, the azide-labeled carbohydrates are promising vibrational probes, suitable for the observation of a broad variety of protein-carbohydrate interactions. As demonstrated, samples can be measured even at low mmol concentrations in H_2O, enabling many future studies of protein-carbohydrate interactions, enzymatic catalysis and glycan structures.

ACKNOWLEDGEMENTS

We acknowledge generous startup funding by the Tenure-Track program of the University of Potsdam and the State of Brandenburg. Research has been supported by the Deutsche Forschungsgemeinschaft (DFG, German Research Foundation) under Germany's Excellence Strategy (EXC 2008/1 – 390540038, UniSysCat, H. M.-W.). Part of the experimental setup and staff are funded by two projects in the EFRE program (European funds for regional development) of the state of Brandenburg, EFRE-InfraFEI (85045645) and EFRE-StaF (85037875).

AUTHOR DECLARATIONS

Disclosures

The authors have no conflicts to disclose.

Author Contributions

P.G. and T.S. contributed equally to this study. P.G. and T.S. performed the IR-experiments and data analysis. P.G., T.S. and H.M.-W. discussed the data and wrote the manuscript. H. M.-W planned and conceptualized the study.

DATA AVAILABILITY STATEMENT

The data that support the findings of this study are available from the corresponding author upon reasonable request.

V. REFERENCES

[1] P. Gasse, T. Stensitzki, Y. Mai-Linde, T. Linker, and H. M. Müller-Werkmeister, "2D-IR spectroscopy of carbohydrates: Characterization of thiocyanate-labeled β-glucose in CHCl3 and H2O," The Journal of Chemical Physics **158**, 145101 (2023).

[2] H. Kim and M. Cho, "Infrared probes for studying the structure and dynamics of biomolecules," Chemical Reviews **113**, 5817–5847 (2013).

[3] R. Feng, M. Wang, W. Zhang, and F. Gai, "Unnatural amino acids for biological spectroscopy and microscopy," Chemical Reviews **124**, 6501–6542 (2024).

[4] M. C. Thielges, "Transparent window 2D IR spectroscopy of proteins," The Journal of Chemical Physics **155**, 040903 (2021).

[5] M. J. Tucker, X. S. Gai, E. E. Fenlon, S. H. Brewer, and R. M. Hochstrasser, "2D IRphoton echo of azido-probes for biomolecular dynamics," Phys. Chem. Chem. Phys. **13**, 2237–2241 (2011).

[6] M. Okuda, K. Ohta, and K. Tominaga, "Vibrational dynamics of azide-derivatized amino acids studied by nonlinear infrared spectroscopy," The Journal of Chemical Physics **142**, 212418 (2015).

[7] J. Y. Park, S. Mondal, H.-J. Kwon, P. K. Sahu, H. Han, K. Kwak, and M. Cho, "Effect of isotope substitution on the Fermi resonance and vibrational lifetime of unnatural amino acids modified with IR probe: A 2D-IR and pump-probe study of 4-azido-L-phenyl alanine," The Journal of Chemical Physics **153**, 164309 (2020).

[8] M. Ruppert, A. Creon, H. Tidow, and N. Huse, "Population Dynamics of Stretching Excitations of p-Azido-phenylalanine Incorporated in Calmodulin–Peptide Complexes," The Journal of Physical Chemistry B **126**, 368–375 (2022).

[9] M. C. Thielges, J. Y. Axup, D. Wong, H. S. Lee, J. K. Chung, P. G. Schultz, and M. D. Fayer, "Two-Dimensional IR Spectroscopy of Protein Dynamics Using Two Vibrational Labels: A Site-Specific Genetically Encoded Unnatural Amino Acid and an Active Site Ligand," The Journal of Physical Chemistry B **115**, 11294–11304 (2011).

[10] P. Pagano, Q. Guo, A. Kohen, and C. M. Cheatum, "Oscillatory Enzyme Dynamics Revealed by Two-Dimensional Infrared Spectroscopy," The Journal of Physical Chemistry Letters **7**, 2507–2511 (2016).

[11] S. Dutta, Y.-L. Li, W. Rock, J. C. D. Houtman, A. Kohen, and C. M. Cheatum, "3-Picolyl Azide Adenine Dinucleotide as a Probe of Femtosecond to Picosecond Enzyme Dynamics," The Journal of Physical Chemistry B **116**, 542–548 (2012).

[12] J. N. Bandaria, S. Dutta, S. E. Hill, A. Kohen, and C. M. Cheatum, "Fast Enzyme Dynamics at the Active Site of Formate Dehydrogenase," Journal of the American Chemical Society **130**, 22–23 (2008).

[13] H. M. Mueller-Werkmeister and J. Bredenbeck, "A donor-acceptor pair for the real time study of vibrational energy transfer in proteins," Physical chemistry chemical physics : PCCP **16** (2014).

[14] X. S. Gai, B. A. Coutifaris, S. H. Brewer, and E. E. Fenlon, "A direct comparison of azide and nitrile vibrational probes," Physical Chemistry Chemical Physics **13**, 5926 (2011).

[15] J.-H. Choi, K.-I. Oh, and M. Cho, "Azido-derivatized compounds as IR probes of local electrostatic environment: Theoretical studies," The Journal of Chemical Physics **129**, 174512 (2008).

[16] J. Y. Park, H.-J. Kwon, S. Mondal, H. Han, K. Kwak, and M. Cho, "Two-dimensional IR spectroscopy reveals a hidden Fermi resonance band in the azido stretch spectrum of β-azidoalanine," Physical Chemistry Chemical Physics **22**, 19223–19229 (2020).

[17] H. Lee, J.-H. Choi, and M. Cho, "Vibrational solvatochromism and electrochromism of cyanide, thiocyanate, and azide anions in water," Physical Chemistry Chemical Physics **12**, 12658 (2010).

[18] A. I. Coelho, G. T. Berry, and M. E. Rubio-Gozalbo, "Galactose metabolism and health:," Current Opinion in Clinical Nutrition and Metabolic Care **18**, 422–427 (2015).

[19] M. E. Taylor and K. Drickamer, *Introduction to glycobiology*, 2nd ed. (Oxford University Press, Oxford ; New York, 2006).

[20] Y.-Y. Zhao, M. Takahashi, J.-G. Gu, E. Miyoshi, A. Matsumoto, S. Kitazume, and N. Taniguchi, "Functional roles of n-glycans in cell signaling and cell adhesion in cancer," Cancer Science **99**, 1304–1310 (2008).

[21] J. L. Johnson, M. B. Jones, S. O. Ryan, and B. A. Cobb, "The regulatory power of glycans and their binding partners in immunity," Trends in Immunology **34**, 290–298 (2013).

[22] B. Imperiali and S. E. O'Connor, "Effect of N-linked glycosylation on glycopeptide and glycoprotein structure," Current Opinion in Chemical Biology **3**, 643–649 (1999).

[23] T. M. Bayless, E. Brown, and D. M. Paige, "Lactase Non-persistence and Lactose Intolerance," Current Gastroenterology Reports **19**, 23 (2017).

[24] P. Hamm and M. Zanni, *Concepts and Methods of 2D Infrared Spectroscopy*, 1st ed. (Cambridge University Press, 2011).

[25] T. Stensitzki, "Skultrafast - a python package for time-resolved spectroscopy," Zenodo (2021).

[26] M. P. Wolfshorndl, R. Baskin, I. Dhawan, and C. H. Londergan, "Covalently Bound Azido Groups Are Very Specific Water Sensors, Even in Hydrogen-Bonding Environments," The Journal of Physical Chemistry B **116**, 1172–1179 (2012).

[27] C. R. Baiz, B. Błasiak, J. Bredenbeck, M. Cho, J.-H. Choi, S. A. Corcelli, A. G. Dijkstra, C.-J. Feng, S. Garrett-Roe, N.-H. Ge, M. W. D. Hanson-Heine, J. D. Hirst, T. L. C. Jansen, K. Kwac, K. J. Kubarych, C. H. Londergan, H. Maekawa, M. Reppert, S. Saito, S. Roy, J. L. Skinner, G. Stock, J. E. Straub, M. C. Thielges, K. Tominaga, A. Tokmakoff, H. Torii, L. Wang, L. J. Webb, and M. T. Zanni, "Vibrational Spectroscopic Map, Vibrational Spectroscopy, and Intermolecular Interaction," Chemical Reviews **120**, 7152–7218 (2020).

[28] S. Dutta, Z. Ren, T. Brinzer, and S. Garrett-Roe, "Two-dimensional ultrafast vibrational spectroscopy of azides in ionic liquids reveals solute-specific solvation," Physical Chemistry Chemical Physics **17**, 26575–26579 (2015).

[29] K.-I. Oh, J.-H. Lee, C. Joo, H. Han, and M. Cho, "β-Azidoalanine as an IR Probe: Application to Amyloid Aβ(16-22) Aggregation," The Journal of Physical Chemistry B **112**, 10352–10357 (2008).

[30] H. M. Müller-Werkmeister, M. Essig, P. Durkin, N. Budisa, and J. Bredenbeck, "Towards Direct Measurement of Ultrafast Vibrational Energy Flow in Proteins," in *Ultrafast Phenomena XIX*, edited by K. Yamanouchi, S. Cundiff, R. de Vivie-Riedle, M. Kuwata-Gonokami, and L. DiMauro (Springer International Publishing, Cham, 2015) pp. 535–538.

[31] E. Lieber, C. N. R. Rao, T. S. Chao, and C. W. W. Hoffman, "Infrared Spectra of Organic Azides," Analytical Chemistry **29**, 916–918 (1957).

[32] I. T. Suydam and S. G. Boxer, "Vibrational Stark Effects Calibrate the Sensitivity of Vibrational Probes for Electric Fields in Proteins," Biochemistry **42**,

12050–12055 (2003).
[33] M. Li, J. Owrutsky, M. Sarisky, J. P. Culver, A. Yodh, and R. M. Hochstrasser, "Vibrational and rotational relaxation times of solvated molecular ions," The Journal of Chemical Physics **98**, 5499–5507 (1993).
[34] D. Czurlok, J. Gleim, J. Lindner, and P. Vöhringer, "Vibrational Energy Relaxation of Thiocyanate Ions in Liquid-to-Supercritical Light and Heavy Water. A Fermi's Golden Rule Analysis," The Journal of Physical Chemistry Letters **5**, 3373–3379 (2014).
[35] J. M. Schmidt-Engler, L. Blankenburg, B. Błasiak, L. J. G. W. van Wilderen, M. Cho, and J. Bredenbeck, "Vibrational Lifetime of the SCN Protein Label in H2O and D2O Reports Site-Specific Solvation and Structure Changes During PYP's Photocycle," Analytical Chemistry **92**, 1024–1032 (2020).
[36] M. Hassani, D. C. Moore, M. G. Roberson, S. Kashid, and M. J. Tucker, "Effects of spectral density on the azide vibrational transition in water versus D2O," Chemical Physics Letters **828**, 140723 (2023).
[37] F. Chalyavi, A. J. Schmitz, N. R. Fetto, M. J. Tucker, S. H. Brewer, and E. E. Fenlon, "Extending the vibrational lifetime of azides with heavy atoms," Physical Chemistry Chemical Physics **22**, 18007–18013 (2020).
[38] P. Hamm, M. Lim, and R. M. Hochstrasser, "Non-Markovian Dynamics of the Vibrations of Ions in Water from Femtosecond Infrared Three-Pulse Photon Echoes," Physical Review Letters **81**, 5326–5329 (1998).
[39] N. T. Hunt, "Using 2D-IR Spectroscopy to Measure the Structure, Dynamics, and Intermolecular Interactions of Proteins in H2O," Accounts of Chemical Research **57**, 685–692 (2024), publisher: American Chemical Society.
[40] B. M. Luther, K. M. Tracy, M. Gerrity, S. Brown, and A. T. Krummel, "2D IR spectroscopy at 100 kHz utilizing a Mid-IR OPCPA laser source," Optics Express **24**, 4117–4127 (2016).
[41] P. Donaldson, G. Greetham, D. Shaw, A. Parker, and M. Towrie, "A 100 kHz Pulse Shaping 2D-IR Spectrometer Based on Dual Yb:KGW Amplifiers," The Journal of Physical Chemistry A **122**, 780–787 (2018).
[42] K. M. Farrell, J. S. Ostrander, A. C. Jones, B. R. Yakami, S. S. Dicke, C. T. Middleton, P. Hamm, and M. T. Zanni, "Shot-to-shot 2D IR spectroscopy at 100 kHz using a Yb laser and custom-designed electronics," Optics Express **28**, 33584–33602 (2020).
[43] P. M. Donaldson, G. M. Greetham, C. T. Middleton, B. M. Luther, M. T. Zanni, P. Hamm, and A. T. Krummel, "Breaking Barriers in Ultrafast Spectroscopy and Imaging Using 100 kHz Amplified Yb-Laser Systems," Accounts of Chemical Research **56**, 2062–2071 (2023), publisher: American Chemical Society.
[44] I. Bhattacharya, J. J. Humston, C. M. Cheatum, and M. Jacob, "Accelerating two-dimensional infrared spectroscopy while preserving lineshapes using GIRAF," Optics Letters **42**, 4573–4576 (2017).
[45] Z. A. Al-Mualem and C. R. Baiz, "Generative Adversarial Neural Networks for Denoising Coherent Multidimensional Spectra," The Journal of Physical Chemistry A **126**, 3816–3825 (2022).

SUPPORTING INFORMATION

A. Transients and decay associated spectra (DAS)

Broadband IR pump-probe data were analyzed with DAS to obtain the vibrational lifetime.

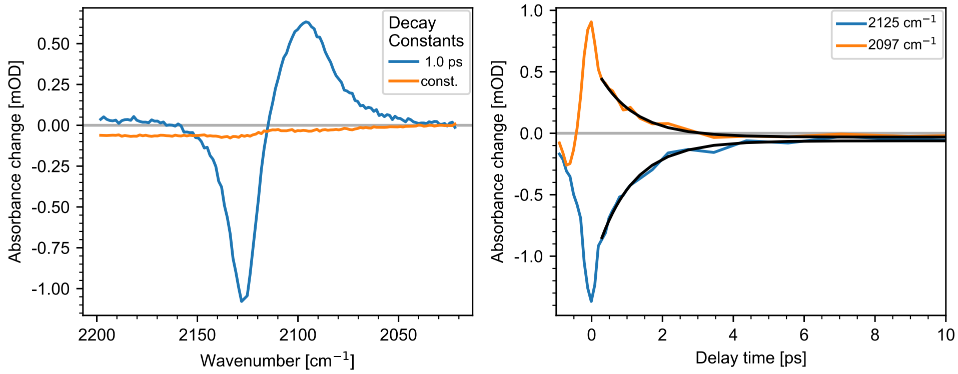

FIG. 1. *Left*: DAS of 1-N_3-GlcNAc. *Right*: Decay of the transient signal of 1-N_3-GlcNAc at 2135 cm^{-1} and 2161 cm^{-1} with the corresponding fit.

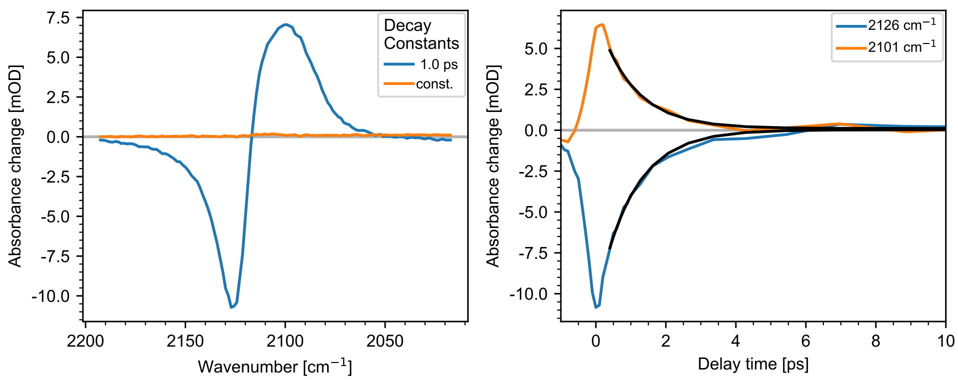

FIG. 2. *Left:* DAS of 1-N_3-Lac. *Right*: Decay of the transient signal of 1-N_3-Lac at 2135 cm^{-1} and 2162 cm^{-1} with the corresponding fit.

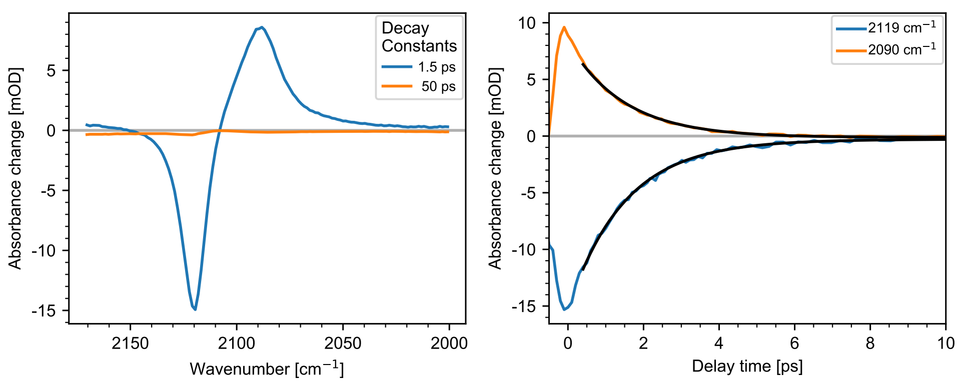

FIG. 3. *Left:* DAS of 2-N_3-Glc. *Right:* Decay of the transient signal of 2-N_3-Glc at 2126 cm^{-1} and 2158 cm^{-1} with the corresponding fit.

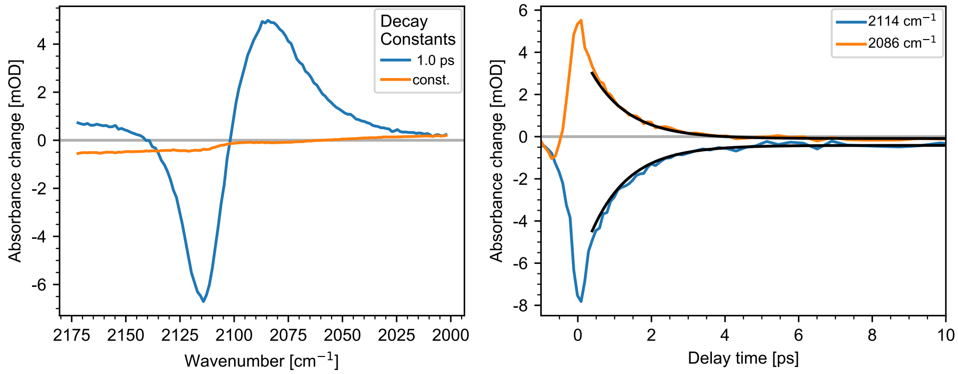

FIG. 4. *Left:* DAS of 6-N_3-Glc. *Right:* Decay of the transient signal of 6-N_3-Glc at 2118 cm^{-1} and 2148 cm^{-1} with the corresponding fit.

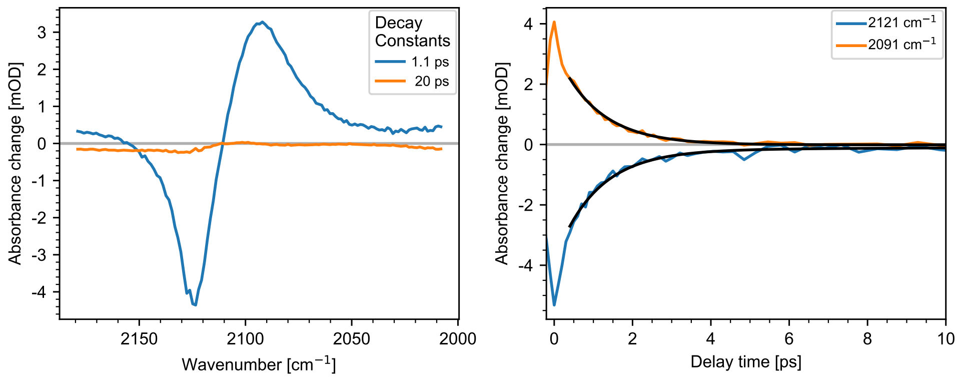

FIG. 5. *Left:* DAS of 6-N_3-Gal. *Right:* Decay of the transient signal of 6-N_3-Glc at 2115 cm^{-1} and 2148 cm^{-1} with the corresponding fit.

B. Artifact reduction in 2D-IR spectra by adjustment of the multiplication factor

When using the normal multiplication factor of 0.5 for the zero-delay between the pump-pulses we observe vertical stripes (see right column below) proportional to the signal. To reduce these artifacts, which we attribute to multi-photon absorption, we adjust the multiplication factor to even smaller values. The used values are given in the table below.

Sample	1-N_3-Lac	1-N_3-GlcNAc	2-N_3-Glc	6-N_3-Gal	6-N_3-Glc
Factor	0.42	0.4	0.35	0.27	0.25

TABLE I. Applied factors of for the multiplication.

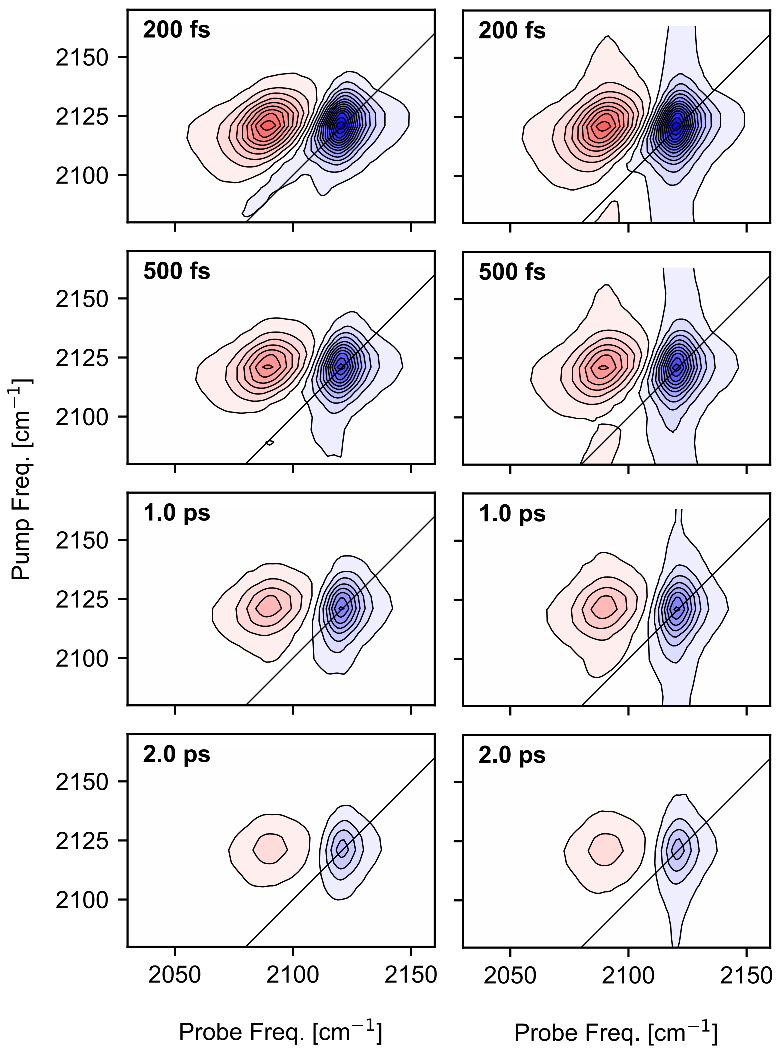

FIG. 6. *Left:* 2D-IR spectra of 2-N_3-Glc with a multiplication factor of the first point at t1 = 0 fs of the interferrogram of 0.35. *Right:* 2D-IR spectra of 2-N_3-Glc with the usual multiplication factor of 0.5.

C. Inhomogeneous line broadening

The following plots show the anti-diagonal (black) and the diagonal slices (red) through the GSB at 150 fs used for the determination of the inhomogeneous line broadening.

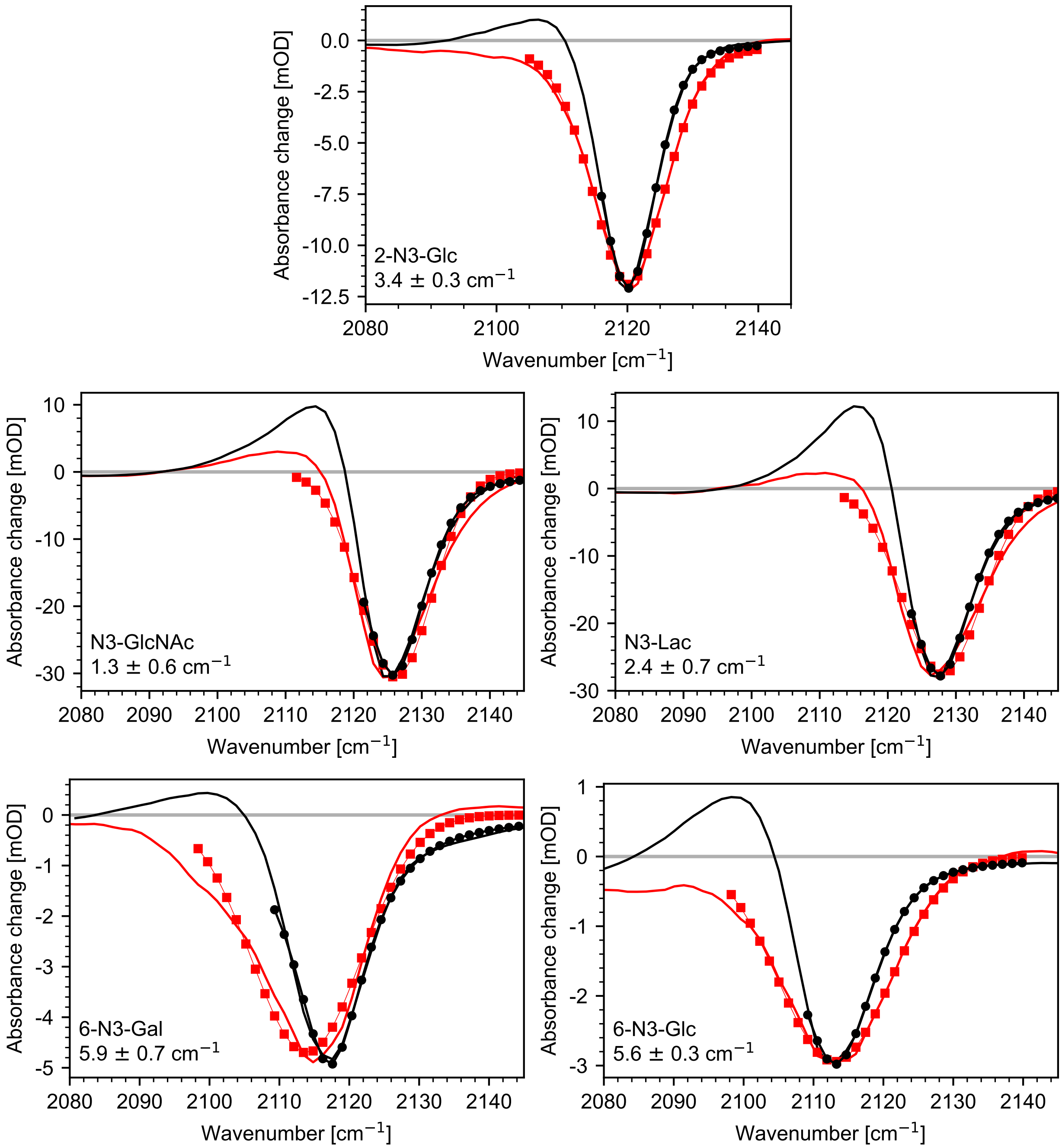

FIG. 7. Lines without a marker showing the diagonal- *(red)* and the anti-diagonal-slices *(black)* of the 2D-spectra at 150 fs. The thin lines with markers show the fit with a pseudo-Voigt function. The resulting were used to calculate the inhomogeneous line broadening shown on the bottom right. As seen in the plot, the fit of the anti-diagonal omits the region at lower wavenumbers to minimize lineshape distortions due to overlap with the positive peak.